ON AN EVOLUTIONARY DEVELOPMENTAL METHODOLOGY FOR PIN-JOINT FRAMEWORK OPTIMIZATION

A THESIS SUBMITTED TO THE GRADUATE DIVISION OF THE
UNIVERSITY OF HAWAI'I AT MĀNOA IN PARTIAL FULFILLMENT
OF THE REQUIREMENTS FOR THE DEGREE OF

MASTER OF SCIENCE

IN

MECHANICAL ENGINEERING

MAY 2019

By
Victor C. Clark

Thesis Committee:

Marcelo Kobayashi, Chairperson
Ronald H. Riggs
Dilmurat Azimov

Keywords: structural topology optimization, L-systems, evolutionary algorithms, trusses

ABSTRACT

The formal investigation into optimal structures, called topology optimization, commenced from the 1904 paper of A.G.M. Michell. While impractical for real constructions, the criteria considered therein allow for a determination of the limit of material economy attainable for truss structures, called Michell structures. These analytical solutions are a useful tool for benchmarking, but have been solved only for a small number of simple cases. The usual computational approaches for identifying these optima rely on a presupposed ground structure, which covers the design space with an initial assemblage of members and joints. While denser ground-structures provide for more refined optima, the stipulation of an initial structure (i.e., topology) artificially restricts the allowable optima.

In the present work, we are concerned with the development and application of a biologically inspired methodology for the study of layout (size, shape, and topology) optimization in pin-jointed frameworks. The methodology is based on the formalism of map L-systems, whose grammar generates purely topological information. This topology is encoded and optimized using an evolutionary algorithm coupled to a non-linear programming method for sizing and shape optimization. Three benchmark test cases are examined which show the gains attainable when a ground-structure is not presupposed.

TABLE OF CONTENTS

LIST OF FIGURES

LIST OF ABBREVIATIONS

LP - Linear Programming (problem)

QP - Quadratic Programming (problem)

NP - Nonlinear Programming (problem)

EP - Evolutionary Programming (problem)

TP - Truss Problem

SLP - Sequential Linear Programming

SQP - Sequential Quadratic Programming

SLSQP - Sequential Least Squares Programming

SNOPT - Sparse Nonlinear Optimizer

CHAPTER 1
INTRODUCTION

Cast into an environment with scattered hazards and food sources, the slime-mold *Physarum polycephalum* will spread from an an initial spore - branching, converging, and culling, as needed - in a manner so as to construct an energy efficient, least path transport network. This property was demonstrated by Tero et al.[1], who placed the mold in an environment modeling Tokyo, its nearby cities, and the surrounding inexorable geographic features. They found the mold's natural organization to rival that of the existing Japanese rail infrastructure in terms of transport efficiency, least total distance covered, and fault tolerance. Particularly remarkable is that no presupposition was made by the initial spore regarding its habitat - no map was given, or destination provided, aside from a primordial knowledge of some ultimate end, for the organism to optimally 'mold' itself to the environment. Such ramified optimization is typical in the development of biological structures, an evolving advantage accompanying the harsh scrutiny of natural competition. Examples are the venation in insect wings[2] and plant leaves[3], which develop through stages: at first in exploration, then as refinement.

Illuminated by such biological processes, Kobayashi [4] pioneered an evolutionary developmental methodology for the study of topology optimization in natural and engineering systems, using a generative grammar system to develop an optimum material distribution for microchip heat cooling, taking inspiration from structural homeostasis mechanisms in plants. This was formally demonstrated in a paper with Pedro and Hude [5], who showed significant gains over existing designs for payload adaptors. It was further developed by Pedro and Kobayashi [6] and applied to optimum lifting surfaces in Kolonay and Kobayashi [7]. The following work is a successor to these endeavors, applied particularly to the search for optimum truss layouts. It seems the first such effort is the conference paper of Allison et al.[8], which provides a useful, independently developed approach for use as a benchmark. In the succeeding, we elaborate on the basic nature of truss structures and their optimum as considered by Michell. A review of the prerequisites occurs in the second chapter: programming, an evolutionary algorithm, and a generative grammar. These are arranged in the third chapter in accordance with the evolutionary programme of Kobayashi. In the final chapter we examine the results of such an application to three benchmark test cases: two cantilevers, and a multiply loaded span.

1.1   Truss Structures

A rod is a straight, prismatic, and linearly elastic mechanical element assigned a cross-sectional area $a \in \mathbb{R}_+$, an elastic modulus $E \in \mathbb{R}^+$, and a length $l \in \mathbb{R}_+$ subject to the requirement $l >> \sqrt{a/\pi}$.
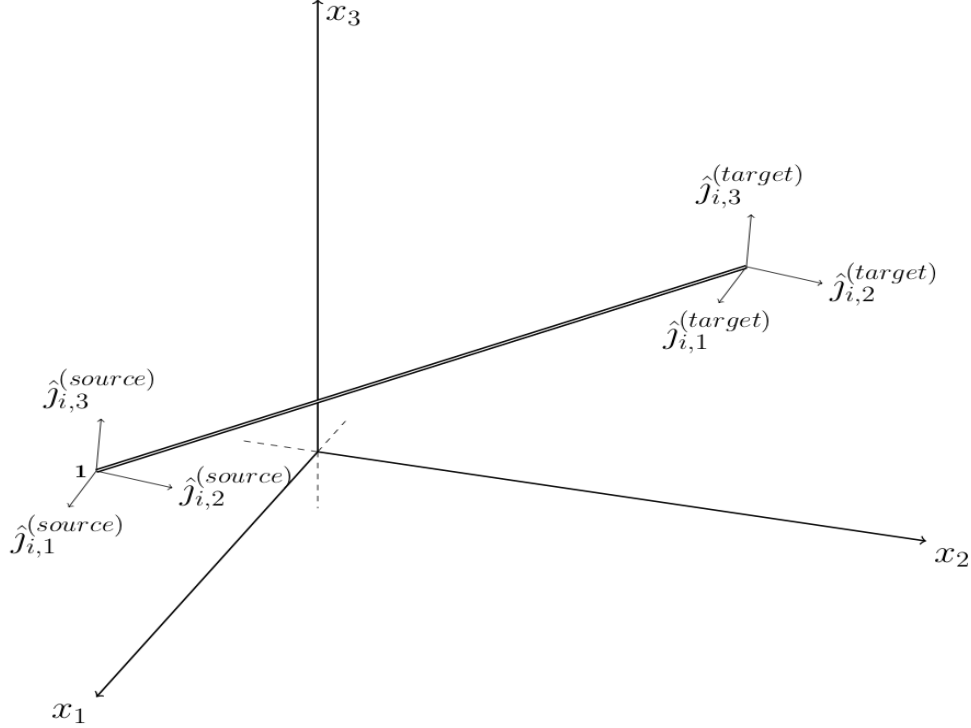
Figure 1.1: Nodal displacement vectors $\hat{\jmath}^{(source)}$ and $\hat{\jmath}^{(target)}$ for member i in three spatial dimensions.

These elements sustain neither couple nor shear, and are static only for pairs of self-equilibrating forces applied at either end of the rod and directed along its length. A truss, or pin-joint framework, is an assemblage of such elements, termed members or connections, joined end-to-end by frictionless pins called nodes, or joints. Each node corresponds to d possible degrees of freedom in the structure, and are the application sites of external loads. Some of these nodes must be restrained (that is, act as the possible load paths to the environment) to achieve equilibrium.

Consider a framework of spatial dimension $d \in \{2, 3\}$ with $j \in \{1, ..., N\}$ nodes and $i \in \{1, ..., m\}$ potential connections. Given $r \geq 3$ many restraints (fixed degrees), there are Nd total global degrees of freedom and $n := Nd - r$ *reduced* global degrees of freedom (free degrees). The use of either global or reduced coordinates is permissible for optimization. Choosing to work with degrees of freedom $p \in \{1, .., n\}$, as in the sequel, allows us to disregard the support reaction forces in member force calculations; geometric considerations generally require a full set $p \in \{1, .., Nd\}$. If the structure is subject to an external loading, $\boldsymbol{f} \in \mathbb{R}^n$, acting on its free degrees, there happens a mobilization of internal forces, $\boldsymbol{t} \in \mathbb{R}^m$, resulting from the elastic response of the m members to internal strains (changes in length) corresponding to effects of the nodal displacements $\boldsymbol{u} \in \mathbb{R}^n$. The applied deformation effort is related to the resulting external deformations through the structures characteristic stiffness, $\boldsymbol{K}$.

To determine the system's global reduced stiffness we define the nodal displacement directions $\hat{j}_{i,k}^{(source)}$, $\hat{j}_{i,k}^{(target)} \in \mathbb{R}^{Nd}$ with $k \in \{1, ..., d\}$, which are the mechanisms for generating strain in member i. Additionally, let the angle between the ith member and kth displacement direction axis be $\varphi_{i,k} \in [0, 2\pi)$. The components of the direction cosine vector $\boldsymbol{\gamma}_i \in \mathbb{R}^n$ for the ith potential member are determined accordingly

$$\boldsymbol{\gamma}_i := [\gamma_i]_p = \begin{cases} \cos \varphi_{i,k} & p = \hat{j}_{i,k}^{(source)} \\ -\cos \varphi_{i,k} & p = \hat{j}_{i,k}^{(target)} \\ 0 & \text{else} \end{cases} \tag{1.1}$$

and so has, at most, $2d$ nonzero elements. Terms *source* and *target* are used arbitrarily to differentiate between the two end nodes of a given member. The stiffness matrix follows in the typical fashion, summing over individual member contributions like

$$\boldsymbol{K} = \sum_{i=1}^{m} a_i \boldsymbol{K}_i = \sum_{i=1}^{m} a_i \frac{E_i}{l_i} \boldsymbol{\gamma}_i \boldsymbol{\gamma}_i^T \tag{1.2}$$

where the base matrices $\boldsymbol{\gamma}_i \boldsymbol{\gamma}_i^T$ correspond to the ith members global response matrix.

Michell Structures

In a celebrated 1904 paper on *The Limits of Economy of Material in Frame-structures*, A.G.M Michell derived sufficient criteria for a structure of least weight, or volume; that is, an *optimum* framework. In particular, he applied the principles of virtual work to a result of Maxwell [9] to arrive at the following conditions: (1) Each member is subject to a tensile (+) or compressive(-) stress equal in magnitude to an allowed stress $\pm\sigma$, and (2) If a virtual deformation is provided satisfying the kinematic constraints the resulting strain in each member is equal in magnitude to a small strain ϵ whose sign agrees with the stress state of the member.

A framework satisfying these conditions is shown to be minimum in volume with respect to all others given the same considerations. Michell further showed that a class of solutions satisfying these criteria are those forming systems of orthogonal curves before and after deformation, and so obeying the strain compatibility

$$\frac{\partial^2 \phi}{\partial \alpha \partial \beta} = 0 \tag{1.3}$$

in two dimensions, where α is a curvilinear coordinate, ϕ is the angle between this this curve and a given fixed direction, and β is a second curvilinear coordinate. Equation (1.3) stipulates that the

minimum structure must lie along the lines of principle strain traced by both systems of curves. In reality, such a structure is not a discrete framework, but a continuum with certain strain properties comparable to an infinite assemblage of infinitesimal elements. Such restrictions (1.3) result in continuous frameworks like that in Fig 1.2, which was found by Michell to have a minimum volume

$$Fa\frac{\pi}{2}\left(\frac{1}{P}+\frac{1}{Q}\right) \tag{1.4}$$

where F is the force applied at midspan, a distance $a = AC = BC$ away from either support, and P and Q are the allowed positive and negative stresses, respectively. These requirements are seen to be the same as those in slip line plastic flow theory, generating Hencky-Prandtl nets. The interested reader is directed to the original work[10] and the succinct report on the subject by A.S.L Chan [11]. An extended treatment is given in the recent text by Lewiński, Sokól, and Graczykowski [12].
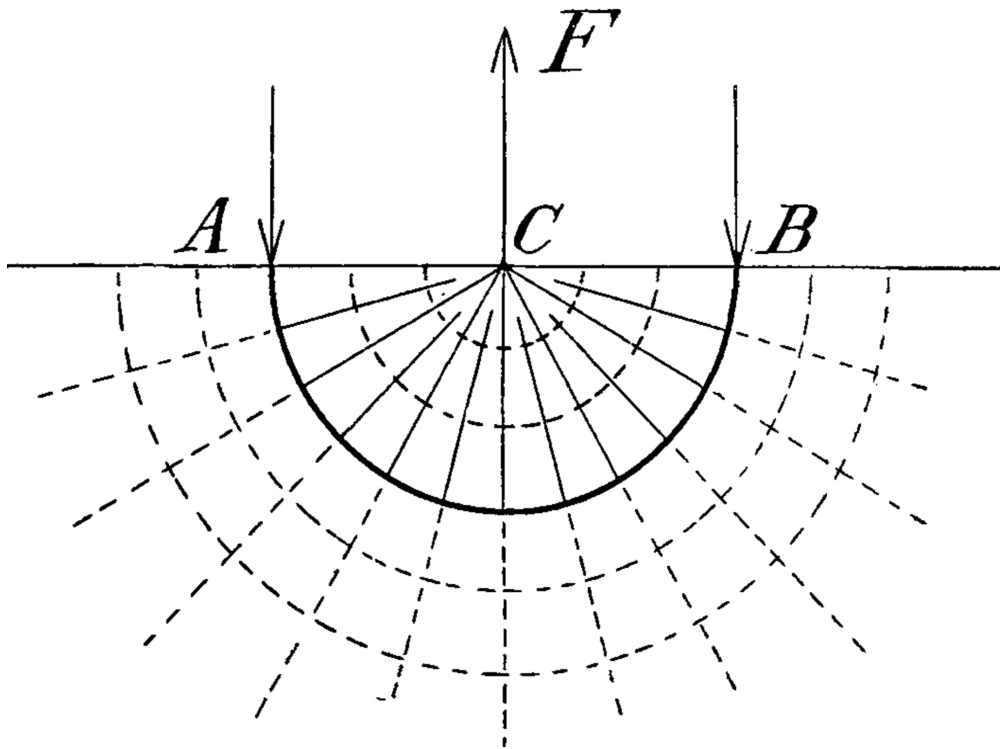

Figure 1.2: Optimum Michell framework for the one load span

4

CHAPTER 2
FOUNDATIONAL METHODS

In the succeeding content we review, in a relatively brief manner, the ingredients for the sequel.

In the first, we investigate two applications of *mathematical programming* to structural topology optimization, the field originating in the work of Michell. For general references see Hemp [13], Christensen and Klarbring [14], or the monograph Bendsøe and Sigmund[15] (see chapters 1, 5 and 4, respectively, for trusses). An instructive set of lectures on the subject is collected by the International Centre for Mechanical Sciences in [16]; of particular relevance are those by Rozvany on exact analytic solutions and their use in numerical validation, and Lewinski and Sokol on the properties of Michell structures. As for technical reviews, see Rozvany and Bendsøe [17] for an extensive review of optimal layout theory of continuous and discrete structures; more recent reviews are [18], highlighting four recent numerical approaches to topology optimization (including Kobayashi's work), [19] on the application of level set method to structural topology optimization, and [20] on the optimization of trusses using discrete valued design variables, focusing extensively on heuristic methods. For an introduction to basic concepts in programming consider the course text developed by Robinson [21].

In the second, we examine the function and composition of a probabilistic optimization scheme termed *genetic algorithms*. The text by Goldberg [22] provides a thorough introduction to these methods; a more digestible overview is given in the 'tutorial' by Mitchell [23]. Applications of genetic algorithms to truss optimization are remarked in [20]. Such a method is considered by Rajan [24], where sizing is accomplished by a linear programming model and staggered shape and topology optimization are achieved through a genetic algorithm using boolean values to indicate connectivity and continuous variables for the permissible - but limited - nodal variations. It should be noted that sizing is chosen from discrete areas values, and that topology is only loosely optimized.

In the third, we explicate the rules of formal grammar systems in general, and in particular the so-called *Lindemeyer grammar systems*. The authoritative text is Prusinkiewicz and Lindenmayer [25], specifically applied to the development of biological systems; a more developed mathematical treatment is presented in [26]. For a general reference on grammars and language see [27] or the works of Chomsky [28] and Chomsky and Miller [29]. Besides the work of Kobayashi and his collaborators [4][5][6][7], the works in engineering are Allison et al., on optimal truss structures [8] and Hartl et al., producing optimal compliant actuating mechanisms for muscular-skeletal structures [30][31]. Other applications of the so-called mapL systems are relegated mostly to the growth and visual modeling of biological structures: see [32] for an application to knot growth and grain

variance in wood, and [33] for fruits and their internal structures. An exception to this is the work of Alber and Rudolph [34] applied to the development and visualization (but not analysis) of 3d frameworks using a graph implementation for the productions that operate on an alphabet containing predefined structural polyhedra parameterized for geometric considerations.

2.1 Mathematical Programming

The term *programming* is meant in the sense of arranging a schedule, or plan, to accomplish some task; *mathematical programming*, then, describes the use of specialized mathematical methods to aid in rigorous optimal decision making. In theory, practitioners hope to obtain some consummate position, the sublime; in practice, theoreticians are seldom able to illuminate that gilded path. Instead, approximate procedures are developed, and the necessary and sufficient conditions (if they exist) are identified, to exploit the mathematical structure of the problem being optimized. For certain classes global, or absolute, optimum are assured. More generally, variational criteria provide the necessary conditions for local optimality, with no guarantees towards sufficiency.

The general optimization *programme* is expressed as the following

$$\min_{\boldsymbol{x} \in S} \quad g(\boldsymbol{x}) \tag{2.1}$$

$$\text{s.t.} \quad h(\boldsymbol{x}) \leq 0 \tag{2.2}$$

where $g : \mathbb{R}^n \to \mathbb{R}$ is an objective function representing some input or output we would like to minimize. We can also maximize this function by negation of the objective results (2.1). If one considers multiple objectives this function becomes vector-valued, whence $g : \mathbb{R}^n \to \mathbb{R}^k$. The modulating, or optimization, variable, $\boldsymbol{x}$, is an element of a given set S, often taken (as herein) to be a subset of $\mathbb{R}^n$. Additional requirements, or constraints, are imposed on the set of admissible solutions by choice of a constraint function $h : \mathbb{R}^n \to \mathbb{R}^m$; that the image is in $\mathbb{R}^m$ means we can consider one, none, or several constraints. These can be of mixed or strict equality/inequality, and need not have the same dependance on the inputs as the objective.

As yet, we have made no more progress than to phrase our problem mathematically: minimize an objective g with respect to the allowable inputs $\boldsymbol{x}$ while adhering to the requirements of h. Depending on our motivation, the basic architecture of (2.1)-(2.2) finds applications in finance, medicine, physics, chemistry and engineering, with the interpretation of $\boldsymbol{x}$, g, and h corresponding to the problem in question. At present, we are concerned with structural optimization: that subset of mathematical programming concerned with distributing load-bearing material in a minimum fashion so as to agree with stress, displacement, buckling, or some other structural criteria. In

particular, we examine the optimal solutions to the usual minimum compliance problem derived from the general equations of elasticity by virtual work

$$\min_{\boldsymbol{u} \in U} \quad \boldsymbol{a}(\boldsymbol{v}, \boldsymbol{u}) \tag{2.3}$$

$$\text{s.t.} \quad \boldsymbol{a}(\boldsymbol{v}, \boldsymbol{u}) = \boldsymbol{l}(\boldsymbol{v}) \tag{2.4}$$

$$\boldsymbol{v} \in U \tag{2.5}$$

seen dual to the problem of minimizing weight in the subsequent. The real ($\boldsymbol{u}$) and virtual ($\boldsymbol{v}$) displacements are taken from the set, U, satisfying kinematic requirements on the boundary. The objective is to minimize the internal virtual strain energy of the deformed body, written here as the typical bi-linear form

$$\boldsymbol{a}(\boldsymbol{v}, \boldsymbol{u}) = \int_{\Omega} \boldsymbol{\nabla} \boldsymbol{v} \boldsymbol{C} \boldsymbol{\nabla} \boldsymbol{u} d\Omega$$

which is synonymous to maximizing the body's stiffness, or minimizing external virtual work of the body forces and surface tractions under a given variation

$$\boldsymbol{l}(\boldsymbol{u}) = \int_{\Omega} \boldsymbol{f} \boldsymbol{u} d\Omega + \int_{\Gamma} \boldsymbol{t} \boldsymbol{u} d\Gamma$$

Linear Programming in Structural Optimization

For linear problems, i.e., those in which the objective function and constraints satisfy additivity[1] and homogeneity[2] with respect to their input, the general formulation (2.1)-(2.2) is clarified as

$$\min_{\boldsymbol{x} \in \mathbb{R}^n} \quad \boldsymbol{c}^T \boldsymbol{x} \tag{2.6}$$

$$\text{s.t.} \quad \boldsymbol{A}\boldsymbol{x} \leq \boldsymbol{b} \tag{2.7}$$

$$\boldsymbol{x} \geq 0 \tag{2.8}$$

such that $\boldsymbol{c}^T$ is a covector of $\boldsymbol{x}$, and $\boldsymbol{A} : \mathbb{R}^n \to \mathbb{R}^m$ is a linear transformation on the admissible set of modulating variables with (possibly nill) image $\boldsymbol{b} \in \mathbb{R}^m$. Unless $m = n$, which guarantees a single solution for nonsingular $\boldsymbol{A}$, we expect non-unique solutions to (2.6)-(2.8).

A ground structure is a presupposed framework specifying both geometry (the relative positions of nodes) and topology (member-node connectivities), which naturally restricts the allowed topologies

[1] $f(u) + f(x) = f(u + x) \forall u, x \in S$
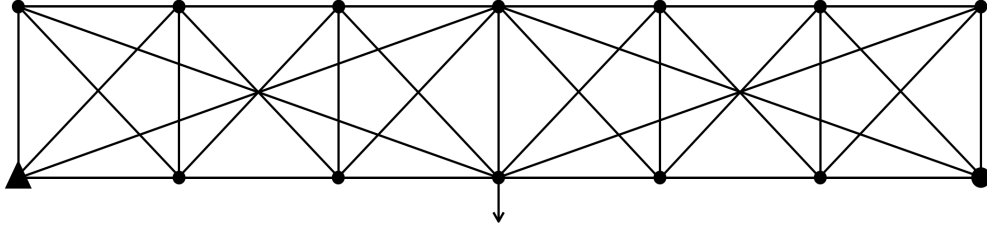[2] $\alpha f(u) = f(\alpha u) \forall u \in S, \alpha \in \mathbb{R}$

Figure 2.1: Possible ground structure for the problem of a one load span.

of the optimized structure (see Fig. 2.1). Using a finite element discretization of (2.3)-(2.5) the compliance optimization problem becomes a sizing problem as well, expressed in the classical form, for fixed geometry

$$\min_{\boldsymbol{a}\in\mathbb{R}^m,\boldsymbol{u}\in\mathbb{R}^n} \quad \boldsymbol{f}^T\boldsymbol{u} \tag{2.9}$$

$$\text{s.t.} \quad \boldsymbol{K}(\boldsymbol{a})\boldsymbol{u} = \boldsymbol{f} \tag{2.10}$$

$$\sum_{i=1}^{m} v_i = V \tag{2.11}$$

$$a_i \geq 0 \tag{2.12}$$

where $\boldsymbol{K}(\boldsymbol{a})$ is the reduced global structural stiffness shown explicitly as a function of the member areas. Objective (2.9) consists of minimizing the compliance in terms of the design variables $\boldsymbol{u}$ and $\boldsymbol{a}$. According to the area bounds (2.9) the truss's topology is allowed to vary only in the sense that a member's area may go to zero. V is a supplied upper bound on the total volume of the structure, and $v_i = a_i l_i$ is the ith member's volume defined by the product of its area, a_i, with its length. If the global stiffness is written in terms of member volumes $\boldsymbol{K}(\boldsymbol{v})$, so $\boldsymbol{K}_i = \sum_{i=1}^{m} \frac{E_i}{l_i^2}\boldsymbol{\gamma}_i\boldsymbol{\gamma}_i^T$ the problem (2.9)-(2.12) is equivalent to a maximization in $\boldsymbol{u}$ subject to nonlinear constraints on the individual member strain energies

$$\max_{\boldsymbol{u}\in\mathbb{R}^n} \quad \boldsymbol{f}^T\boldsymbol{u} \tag{2.13}$$

$$\text{s.t.} \quad \boldsymbol{u}^T\boldsymbol{K}_i\boldsymbol{u} \leq 1 \tag{2.14}$$

where, for a positive semidefinite[3], symmetric $\boldsymbol{K}(\boldsymbol{v})$, which is the case, we can use the decomposition

---

[3]A matrix, $\boldsymbol{K}$, is positive definite if $\boldsymbol{x}^T\boldsymbol{K}\boldsymbol{x} > 0$ for all $\boldsymbol{x} \neq \boldsymbol{0}$. A positive semidefinite matrix is one which loosens the restriction on inequality to allow $\boldsymbol{x} = \boldsymbol{0}$. This is reasonable, lest we expect our structure to decrease in internal energy under deformations from an unstrained reference.

$uK_iu = \left(\frac{\sqrt{E_i}}{l_i} \gamma_i^T u \right)^2$ to arrive at an **LP** formulation of the minimum compliance problems in terms of u alone[15][35]

$$\max_{u \in \mathbb{R}^n} \quad f^T u \tag{2.15}$$

$$\text{s.t.} \quad -1 \leq \frac{\sqrt{E_i}}{l_i} \gamma_i^T u \leq 1 \tag{2.16}$$

This problem admits an equivalent **LP** formulation in terms of slack variables t' and t''

$$\min_{t', t'' \in \mathbb{R}^m} \quad \sum_{i=1}^{m} (t_i' + t_i'') l_i \tag{2.17}$$

$$\text{s.t.} \quad \sum_{i=1}^{m} \sqrt{E_i}(t_i'' - t_i')\gamma_i + f = 0 \tag{2.18}$$

$$t_i', t_i'' \geq 0 \tag{2.19}$$

where, if we make the substitution $t_i = \sqrt{E_i}(t_i'' - t_i')$ for the ith member force and $a_i = (t_i' + t_i'')$ for the corresponding member's area, we find that (2.15)-(2.16) is equivalent to a minimization of the volume, constrained by static requirements and stress conditions

$$\min_{a \in \mathbb{R}^m} \quad \sum_{i=0}^{m} a_i l_i \tag{2.20}$$

$$\text{s.t.} \quad \sum_{i=0}^{m} t_i \gamma_i + f = 0 \tag{2.21}$$

$$-\sqrt{E_i} a_i \leq t_i \leq \sqrt{E_i} a_i \tag{2.22}$$

which is Hemps linear programming formulation of Michell's problem with the scaling $\sigma_i = \sqrt{E_i}$. By duality in linear programming, a global optimum is guaranteed satisfying both (2.15)-(2.16)
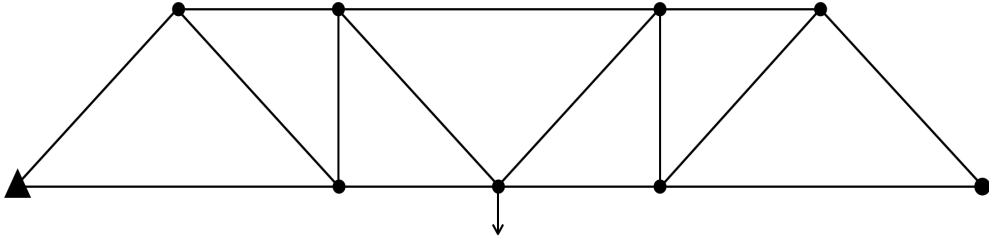

Figure 2.2: LP solution to the one load span using the ground structure in Fig 2.1.

and (2.20-2.22), though it need not be unique. This makes sense if we reflect that $\epsilon_i = l_i^{-1}\boldsymbol{\gamma}_i^T\boldsymbol{u}$, so both of Michell's criteria are reflected in the dual formulations. Numerical solutions to (2.17)-(2.19) are easily determined using Danzig's simplex algorithm. For example, applying **LP** to the ground structure in Fig 2.1 gives the optimum shown in Fig 2.2 with a volume $V_{LP} = 16.0$. Using $F = Q = P = 1$ and $a = 3$, (1.4) gives a volume $V_{min} = 3\pi \approx 9.4248$, which is significantly lower than the **LP** value. In the subsequent we extend this to a framework in which an initial ground topology is stipulated, but the spatial positions of the unrestrained nodes are allowed to vary.

Nonlinear Programming in Structural Optimization

To this end, we consider the complete set of nodal coordinates in the non-reduced system, which are again N many. If $p \in \{1, ..., Nd\}$, corresponds to a possible degree of freedom the initial nodal positions can be collected in $\overline{\boldsymbol{y}} \in \mathbb{R}^{Nd}$. If $k \in \{1, ..., d\}$ the component $\overline{y}_p$ corresponds to the kth component of node j's position. Obtainable geometries are specified by a choice of a set $Y \subset \mathbb{R}^{Nd}$, such that $\boldsymbol{y} \in Y$ is a vector of allowed nodal positions. Problem (2.9)-(2.12) naturally generalizes to include these changing geometries

$$\min_{\boldsymbol{a}\in\mathbb{R}^m,\boldsymbol{u}\in\mathbb{R}^n,\boldsymbol{y}\in Y} \quad \boldsymbol{f}^T\boldsymbol{u} \tag{2.23}$$

$$\text{s.t.} \quad \boldsymbol{K}(\boldsymbol{a},\boldsymbol{y})\boldsymbol{u} \;=\; \boldsymbol{f} \tag{2.24}$$

$$\sum_{i=1}^{m} a_i l_i(\boldsymbol{y}) \;=\; V \tag{2.25}$$

$$a_i \;\geq\; 0 \tag{2.26}$$

The admission of this nodal design variable affects the problem data in several ways, and may furnish added difficulty with regards to the phenomena of so-called 'melting nodes'. As the end nodes of a given member are modulated the angle $\varphi_{i,k}(\boldsymbol{y})$, which member i makes with respect to axis k, changes. By this consideration so too does the direction cosine vector, $\boldsymbol{\gamma}_i(\boldsymbol{y})$. The individual member lengths are dependent on y in a more direct fashion, like

$$l_i(\boldsymbol{y}) = \sqrt{\sum_{k=1}^{d} \left(y_{\hat{\jmath}_{i,k}^{(target)}} - y_{\hat{\jmath}_{i,k}^{(source)}} \right)^2}$$

where two nodes are considered melting if $y_{\hat{\jmath}_{i,k}^{(source)}} = y_{\hat{\jmath}_{i,k}^{(target)}} \; \forall k$, or $l_i(y) = 0$.

While the presence of melting nodes is crucial to limiting the number of bars, they may also form a singularity in the model, manifest in two ways: the function $l_i(\cdot)$ ceases to be differentiable for

such geometries, and the global stiffness matrix becomes singular. To overcome these difficulties, Achtziger[36] provides an alternate evaluation for the functions $l_i(\cdot)$ and $K(\cdot, \cdot)$ as follows:

For each spatial dimension k, define a vector

$$\boldsymbol{v}_i^{(k)} := [v_p^{(k)}]_i = \begin{cases} 1 & p = \hat{j}_{i,k}^{(source)} \\ -1 & p = \hat{j}_{i,k}^{(target)} \\ 0 & \text{else} \end{cases}$$

associated with the ith member whose Nd elements beget the matrix

$$\boldsymbol{C}_i := \sum_{k=1}^{d} \boldsymbol{v}_i^{(k)} \left(\boldsymbol{v}_i^{(k)}\right)^T \tag{2.27}$$

where $\boldsymbol{C}_i \in \mathbb{R}^{Nd} \times \mathbb{R}^{Nd}$. The projection matrix, $\boldsymbol{P} \in \mathbb{R}^n \times \mathbb{R}^{Nd}$ is defined

$$\boldsymbol{P} = \left(1_{n \times n} \; 0_{n \times s}\right) \tag{2.28}$$

so that when it left multiplies a vector with Nd elements the first $p = 1, ..., n$ are retained, and the remaining, restrained degrees $p = n+1, ...Nd$ are nullified. In particular, these allow for the substitutions $l_i(\boldsymbol{y}) = \boldsymbol{y}^T \boldsymbol{C}_i \boldsymbol{y}$ and $\boldsymbol{\gamma}_i = \frac{1}{l_i(\boldsymbol{y})} \boldsymbol{P} \boldsymbol{C}_i \boldsymbol{y}$. If a node melts we have $\boldsymbol{y}^T \boldsymbol{C}_i \boldsymbol{y} = 0$, which implies $\boldsymbol{C}_i \boldsymbol{y} = \boldsymbol{0}$. The denominator of $\boldsymbol{\gamma}_i$ is addressed by a suitable change of variables.

Using similar manipulations to those yielding the linear programming problem (2.17)-(2.19), we
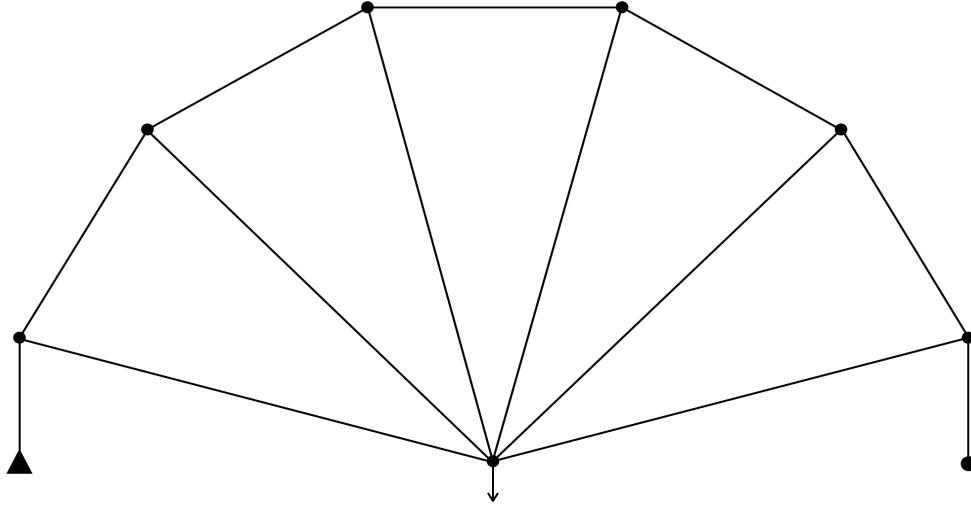

Figure 2.3: NP solution to the one load span using the ground structure in Fig 2.1.

arrive at a nonlinear programming (**NP**) form for simultaneous member size and truss shape optimization

$$\min_{\substack{\mu,\lambda \in R^m \\ y \in Y}} \quad \sum_{i=1}^{m} \left(t_i' + t_i''\right) \boldsymbol{y}^T \boldsymbol{C}_i \boldsymbol{y} \tag{2.29}$$

$$\text{s.t.} \ \sum_{i=1}^{m} \sqrt{E_i}\left(t_i'' - t_i'\right)\boldsymbol{PC}_i\boldsymbol{y} + \boldsymbol{f} = \boldsymbol{0} \tag{2.30}$$

$$t_i', t_i'' \ \geq \ 0 \tag{2.31}$$

which is seen to be cubic in the objective function and quadratic in the dynamic constraints. If we reassert the change of variables $a_i = (t_i' + t_i'')l_i(\boldsymbol{y})$ and $t_i = \sqrt{E_i}(t_i'' - t_i')l_i(\boldsymbol{y})$ we recover a similar minimum volume expression to (2.20)-(2.22). Solutions $(\boldsymbol{t}', \boldsymbol{t}'', \boldsymbol{y})$ to this problem are guaranteed in a "local-global-global" sense as a global solution is guaranteed for the linear problem given a fixed geometry. Approximate solutions satisfying the necessary first-order Karush-Kuhn-Tucker (KKT) conditions are readily found using the method of sequential quadratic programing (SQP). Applying **NP** to the ground structure of Fig 2.1 gives the framework in Fig 2.3, which has a volume $V_{NP} = 9.6462$ and whose height is the same as the length of the mid span length, a. This result is much closer, both in volume and semi-circular/radial configuration, to the optimum predicted by Michell in Fig 1.2.

2.2   Genetic Algorithms

The numerical optimization techniques for nonlinear problems based in calculus are generally of two kinds: one can search for extremals of the objective function by setting its variation equal to zero; otherwise, one travels the path of steepest decent/ascent from an initial point in steps whose directions are determined by the gradient, hessian, or similar, calculated anew at each step. Depending on the choice of initial input, the optima obtained by these methods are only guaranteed in a local sense. Genetic algorithms (GAs) are evolutionary inspired computational schemes for nonlinear, and possibly constrained, optimization. They distinguish themselves from calculus based methods in that they (1) employ stochastic transition rules, (2) consider entire collections, or populations, of inputs in parallel, (3) work with genotypical representations (a set of parameters) instead of directly with the phenotype (the parameterized modulation variables), and (4) use only the objective information resulting from (2) to progress towards the global optimum.

From evolutionary and genetic terminology, a population is a collection of individuals, or chromosomes, each encoded by an ordered set of genes. An individual represents a trial solution,

which is assigned a fitness value corresponding to the assessment of some fitness function, i.e., the objective function. The chromosome encoding is chosen such that the allowable values of x are representable, say by a finite array of parameters, a_m. These parameters are typically converted into a single binary string

$$ind = [a_1, a_2, ..., a_m] = b_1 b_2 b_3 ... b_{n-2} b_{n-1} b_n$$

For example, if we seek to minimize the function $f : B \rightarrow \mathbb{R}$ whose integer valued range is given by $f(x) = \{(x-3)^2 | x \in B\}$, where $B = \{-15, -14, ...0, ..., 14, 15\}$, we might consider an initial population of individuals with two genes encoded in a 5-bit string, the first serving to indicate the sign, and the second demonstrating the decimal magnitude of the number

$$pop = [[+, 12], [-, 9], [+, 3], [+, 0], [+, 5], [-, 7]]$$
$$= [01100, 11001, 00011, 00000, 00101, 10111]$$

Operators

Successive generations from the initial population are generated by applying three specialized evolutionary operators (selection, crossover, and mutation), and then applying them again for all subsequent generations, save for the last. While their specific implementation may vary, the thrust of these methods is to manipulate the chromosomal information of an initial population over generations towards a more desirable/advantageous gene pool.

Selection describes the process of choosing genetic, or chromosomal, information to pass on to succeeding generations, say by specifying a probability distribution correlating an individuals fitness to its reproductive attractiveness, or by some other means of discriminating the less fit individuals from the more competitive ones. This is applied in such a way as to preserve the current generation, meaning an individual, or individuals, can be selected to reproduce multiple times in a given generation. The resulting offspring from such pairings are determined by the next operator.

The crossover operation is analogous to genetic recombination, using two of the selected chromosomes (parents) to produce two novel chromosomes with traits from both of the originals. For example, using the first two individuals of the previously enumerated population, a single point crossover might yield
$$(011|00, 110|01) \rightarrow (110|00, 011|01)$$

and a two point crossover
$$(01|10|0, 11|00|1) \rightarrow (11|10|1, 01|00|0)$$

A mutation operator can be applied before or after the crossover operation, and usually amounts to

flipping one or more of the bits in the concerned individual. The purpose of this operator is preserve a certain genetic diversity within the system, which is needed to avoid premature convergence and allows for a broader exploration of the design space. We note that a specific generation can only be said to be more 'fit' than the ones considered prior. If the initial population lacks a variance in genetic information, the reproductive ingenuity of succeeding generations is limited, or biased towards certain results. By introducing random mutations to the chromosomal information of a population one hopes to limit the effects of inbreeding, which in a GA results from considering the offspring of a prior generation as the reproductive group generating future offspring. This can also be helped by providing a large initial population.

2.3   L-system Grammars

In the late 1960's the theoretical biologist, Aristid Lindemeyer, demonstrated the efficacy of a novel string rewriting formalism to consider branching and dividing topologies in natural structures, namely those in plants and simple multi-cellular organisms. These grammar systems, termed Lindemeyer systems, or L-systems, are distinct from those described by Chomsky in that their production rules are applied in parallel, as opposed to in sequence, reflecting their original biological intent. This formalism was initially described in terms of sequential machines, which consider inputs to states generated by prior inputs to states whose origin are an initial input to an initial state[37]. Modern descriptions of L-systems borrow from the terminology made standard in the study of formal grammars.

We begin with an alphabet, Σ, which is a finite nonempty set whose elements are referred to as letters, or symbols. Any two of these elements, say $x, y \in \Sigma$, can be joined like so

$$x \wedge y = xy \tag{2.32}$$

with the non-commutative concatenation operator, $\wedge$. The empty element, λ, is such that $\lambda x = x\lambda = x \ \forall x \in \Sigma$. Catenation of any two elements in Σ generates an element of the set Σ^2. Elements of this new set can be catenated with elements of Σ to generate Σ^3, and so on. For example, if we take $\Sigma = \{\lambda, 0, 1\}$ then $\Sigma^2 = \{\lambda, 0, 1, 00, 01, 10, 11\}$ and $\Sigma^3 = \{\lambda, 0, 1, 00, 01, 10, 11, 000, 100, 010, 011$ $110, 101, 111\}$. In general

$$\Sigma^k := \{w_1...w_m | w_1 \in \Sigma^{n_1}, ..., w_m \in \Sigma^{n_m}, n_1 + ... + n_m = k\} \tag{2.33}$$

from which we determine $\wedge : \Sigma^{n_1} \times ... \times \Sigma^{n_m} \to \Sigma^{n_1 + ... + n_m}$. A word then, or string, is any $w \in \Sigma^k$ for $k \geq 0$, but is typically reserved $\forall k \geq 2$. A letter is the special case of $k = 1$ - i.e., an element

of the root alphabet. The reapellated *empty-word*, λ, is the sole element for $k = 0$. While Σ is finite, catenations in the limit $k \to \infty$ produce a countably infinite monoid - the set of all words, or strings, over Σ - designated Σ^*. The associated semi-group is Σ^+, which is the set of all nonempty[4] words over Σ. Note the order k may be arbitrarily extended by the insertion of the empty word.

A string 0L-system then, is a triple, $G = (\Sigma, \omega, P)$, where Σ is as above, $\omega \in \Sigma^+$ is an initial generator called the axiom, or seed, and $P \subset \Sigma \times \Sigma^*$ is a collection of productions. A production, written $x \to \chi$, is a couple, $(x, \chi) \in P$, where $x \in \Sigma$ and $\chi \in \Sigma^*$. Each $x \in \Sigma$ is assumed to have a production associating it to a particular χ - identity, $x \to x$, if a unique production is not specified. For words $\alpha, \beta \in \Sigma^*$, parallel rewriting is realized by $\alpha \Longrightarrow_G \beta$ iff $\alpha = x_1...x_k$, $\beta = \chi_1...\chi_k$, and $(x_i, \chi_i) \in P$ for each $i \in \{1, ..., k\}$. Given the transitive, reflexive closure of $\Longrightarrow_G$, the language (or set of all words) generated by G is $L(G) := \{\nu \in \Sigma^* | \omega \Longrightarrow_G^* \nu\}$. We denote the succession of topologies generated by acting the set productions P on the axiom ω, and its successors, with ω_n; by definition, $\omega_o = \omega$.

To elucidate this formalism consider the L-system composed of $\Sigma = \{0, 1\}$, $P = \{0 \to 000, 1 \to 101\}$, and $\omega = 1$. According to the axiom, application of the productions to ω_n begets the sequence

$$1$$
$$101$$
$$101000101$$
$$101000101000000000101000101$$
$$101000101000000000101000101000000000000000000...$$

and so on, generating the Cantor set if we identify 1 with a line segment, and 0 and all successors (000) with a deletion of the middle third of said line segment. Alternatively, using the same alphabet

---

[4]$\Sigma^+ := \Sigma^* - \{\lambda\}$

but taking $P = \{0 \rightarrow 01, 1 \rightarrow 0\}$ and $\omega = 0$, application of the productions to ω_n yields

$$0$$
$$01$$
$$010$$
$$01001$$
$$01001010$$
$$0100101001001$$

and so on, and is referred to as the Fibonacci series L-system due to the occurrence count of the axiom at each step: 1, 1, 2, 3, 5, 8,... etc.

map L-systems

As per their original motivation, a map is synonymous with a cellular layer. The individual cells are regions enclosed by a finite set of walls, or edges, meeting at vertices. Regions are connected in the sense that there are no cellular voids; all regions within the map correspond to cells. Edges are connected to each other at vertices, and are labeled and assigned a directionality. Division of a region, understood similarly to cellular replication, is binary, either producing two 'daughter' regions or returning the same 'parent' region. This process is assumed to propagate, meaning regions can neither fuse nor disappear - once a region, always a region.

A Binary Propagating Map 0L system with markers, shortened mBPM0L system, is a collection $\mathcal{G} = (\Sigma, \Gamma, \omega, P)$ where Σ is an alphabet consisting of edge labels, $\Gamma = \{\lambda, \rightarrow, \leftarrow, +, -, [,]\}$ is the set of allowable markers, ω is an initial map with edge labels and markers from Σ and Γ, respectively, and P is a set of edge productions, which are applied in parallel to all labels of an axiom. An edge assigned a label, say $A \in \Sigma$, can either be left $\overleftarrow{A}$ or right $\overrightarrow{A}$ directed, or can remain neutral A, though these will not be considered in the sequel. Map division is accomplished by applying, in parallel, the production rules, which behave like $A \rightarrow \alpha$, mapping a neutral or directed predecessor $A \in \Sigma_m$ to a successor edge $\alpha \in \Sigma_\Gamma^*$ comprised of a string of concatenated, marked, edge labels, $\Sigma_m = \Sigma \times \{\lambda, \rightarrow, \leftarrow\}$ and $\Sigma_\Gamma = \Sigma \times \Gamma$.

The inclusion of marked labels, delimited by [and], in a successor indicates the potential of an edge to branch and develop a novel edge (so two novel regions), and is realized from branch to edge only if an edge on the boundary of an adjacent region provides a compatible connection site. The labels in the successor outside these delimiters stipulate the relabeling of the predecessor. Enclosed

$$\omega = \vec{A}x\vec{B}$$
$$\vec{A} \to \vec{B}[+\vec{A}]x$$
$$\vec{B} \to x[+\overleftarrow{A}]x$$
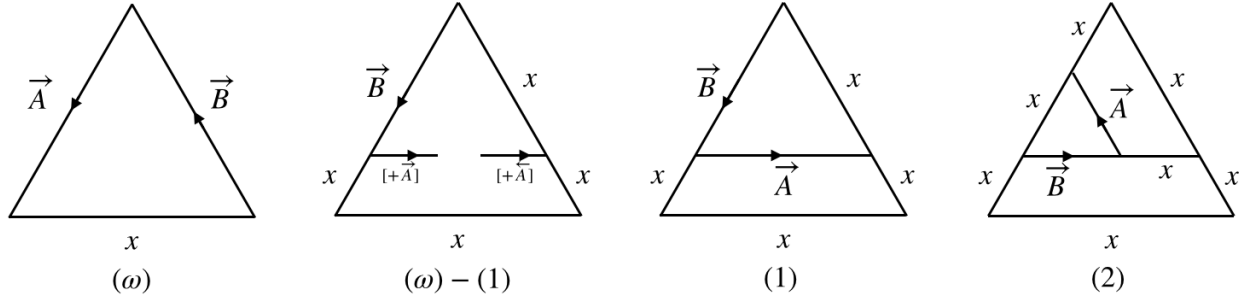
Figure 2.4: A simple map L-system and the first two topologies resulting from applying the productions to the axiom ω.

within each delimiting pair are two symbols. The first is a +, or −, which indicates whether the branch is added to the left or right of the predecessor, depending on its directionality. The second is a directed edge label, marked either by →, showing the branch points away from the successor, or ←, showing the opposite. Branches are considered compatible if they are in the same region, share the same edge label, and are directed in such a way that joining them produces an edge with a single, coherent direction.

For example, consider the development of the axiom $\vec{A}x\vec{B}$ in Figure 2.2, which defines the initial map of an L-system constructed from the alphabet $\Sigma = \{A, B, x\}$. Applying the listed production, the edge marked $\vec{A}$ is relabeled $\vec{B}[+\vec{A}]x$, where the prospective branch $[+\vec{A}]$ is positioned on the left side of (+), and directed away from (→), the predecessor. The production for $\vec{B}$ is similar, only with its branch directed towards the predecessor, allowing for the creation of a novel edge $\vec{A}$. Applying these again yield (2), and so on.

17

CHAPTER 3
EVOLUTIONARY DEVELOPMENTAL METHODOLOGY

As suggested in the prequel, the **LP** and **NP** problems are efficient local optimizers. Given an initial ground structure, and the desired material limitations, the **LP** form guarantees a solution for both statically determinate and statically indeterminate truss structures. The existence of such solutions are, in part, due to a duality criterion in linear programming which stipulates that a solution to minimization problem is an optimum only if it is also the solution to a corresponding maximization problem, but more specifically through their satisfaction of Michell's criteria. If the problem is convex the global optimum is easily obtainable. Otherwise, one expects either non-unique solutions, say a minimum volume that is attainable by several layouts, or a multitude of local optima, or volumes, such that a global optimum is not readily discernible. The **NP** form provides a more robust search as concerns minimum volume trusses, allowing for the structure's geometry to be considered in concert with individual member sizing. As with the linear problem, various optima are attainable, each of which will typically satisfy the first order KKT conditions.

A restriction to either approach is that they can only loosely be interpreted as optimizing the topology - that is, by allowing members to vanish from the framework. Those members whose areas shrink to zero are neglected from dynamic considerations, but are such that they may reappear, as required, to bear load. This is to say that an initial topology is defined for the structure such that the subsequent obtainable, or allowable, topologies are understood to be subsets of the original. For the nonlinear case, melting nodes provide another avenue for topology optimization, in particular individual members may vanish ($l_i = 0$) or reemerge ($l_i = 0 \rightarrow l_i \neq 0$). This annihilation, or generation, is restricted, however, because only those predefined members are allowed to participate in the design-space search.

Either means of topology optimization (vanishing areas and melting nodes) suffer from the same limitation: they rely on a predefined topology, and therefore are limited in which optimum can ultimately be expressed. As per Michell's observation, an optimum framework is optimum only with respect to the set of possible frameworks considered. To determine the ideal structure we must consider all those structures satisfying the required dynamic and stress constraints. In the continuum limit, the entire design space can be actualized. Such a structure would require members on the order of infintesimal lengths, which is impractical for actual truss constructions. Instead, one generally considers a finite, discretized search space: a ground structure. An increasingly dense and connected ground structure can approximate a continuous design space, yet the computational resources required to do so are correlated with the level of refinement. For example, analyzing a problem with twice the aspect ratio of a similar, original problem, would require at least twice as

many design variables to maintain the same ground structure density. Generally speaking, a more refined ground structure will also produce an overabundance of redundant design variables, which can add undesired, unwarranted, complexity.

The proposed methodology seeks to avoid these shortcomings, providing a novel program for identifying optimal truss layouts - that is, simultaneous size, shape, and topology optimization, without the precondition of a ground structure. This approach works in tandem: a **GA** is encoded to explore pure topological information using the formalism of map L-systems and a subordinate program exploits this information and configures the trusses' geometry and material allocation according to **NP**. To start, we require a simply connected geometry of three or more line segments, termed the initial map in the sense of an L-system. This topological construct is discretized to be compatible with later geometric considerations and assumes that possible connections are realized by (straight) lines. Assigning to each edge a marked label from an alphabet, Σ, begets an axiom, ω. By specifying a set of productions and applying them in parallel a given number of times we generate a novel topology from the initial map. In a post processing step the developed topology is provided a more specific geometry: map vertices become nodes and are given a location, and connections become members with determined length. This information is provided to the **NP** form and the optimum volume, if it exists, is approximated.

For the remainder, the initial map is chosen such that predetermined vertices correspond to restraint and load sites in the problem. This need not be the case - various approaches can be employed to mobilize vertices in the bulk as support or load sites, either though direct implementation, or by exploiting the geometrical symmetries of a problem. Note that by specifying an initial we have not pre-determined those obtainable topologies; instead, this consideration influences the dynamics of cellular and evolutionary development[1]. Consequently, this map exists in a gradation between Michell's upper bound (a finite design space with finite boundary) and lower bound (an unbounded, continuous design space), as we can stretch and refine the topology as desired. It remains to determine, provided some map, which axiom and productions (which grammar) should be supplied to develop the topology of an optimum structure. In the sequel we will refer to this methodology as Evolutionary Programming **EP**, for brevity.

3.1   Genetic Implementation

We would like to optimize a truss problem (**TP**) with s supports and p applied loads. First, connect these by a convex polygon of degree at least $n \geq s + p \geq 3$ to construct a map ϖ. Set an alphabet

---

[1]That is, how the topology grows over successive application of productions, and the paths investigated by the the coupled **GA**.

$\Sigma := \{\lambda, 0, ..., \eta_{nt} - 1\}$, where η_{nt} is a set number of non-terminal tokens. A trial candidate for $\mathbf{TP}_\varpi$ is constructed like

$$a_{candidate}^\varpi = [\eta_{dc}, \omega, P] \tag{3.1}$$

where η_{dc} is the number of developmental cycles, which are applications of the production rules. The axiom, $\omega \in \Sigma^*$, is generated by assigning a marked label to each of the maps edges taken from $\{0, ..., \eta_{nt}\}$. Production rules $P = [P_0, ..., P_{\eta_{nt}-1}]$ are like those described for map L-systems, and are applied to the axiom η_{dc} many times. Passing the resulting topology to $\mathbf{NP}$ yields an optimum volume $V_{candidate}^\varpi$ which is, for all intents, determined, up to the attainable minima of $\mathbf{TP}_\varpi$, according to $a_{candidate}^\varpi$. These genetic attributes are readily encoded in a binary string such as

$$a_{candidate}^\varpi = b_1^{(\eta_{dc})}...b_{\eta_1}^{(\eta_{dc})}b_1^{(\omega)}...b_{\eta_2}^{(\omega)}b_1^{(P)}...b_{\eta_3}^{(P)} \tag{3.2}$$

where η_{dc} is relegated to a $\eta_1 = 4$ bit representation, providing for (at most) seventeen developmental cycles. In other words, we consider $\eta_{dc} = (2 + (b_1...b_4)_2 \bmod m_1)$ possible divisions, with $b_i \in \{0, 1\}$ and $1 \leq m_1 \leq (10000)_2 = 16$. A minimum $\eta_{dc} \geq 2$ is required so that progress is made away from the axiom; the maximum number is set by choosing a value $m_1 \in \mathbb{N}$ at most one greater than the maximum value expressed by η_1 bits. For example, if $m_1 = 3$ there are six ways to obtain $\eta_{dc} = 2$ and five to obtain $\eta_{dc} = 3$ or $\eta_{dc} = 4$. Depending on the level of refinement we might insist on a larger m_1, expanding the bit count as needed; that is, choosing $m_1 \geq 17$ has no effect for $\eta_1 = 4$. The axiom is stored in $\eta_2 = 17n$ bits, seventeen for each element, or label. Directionality $(\rightarrow, \leftarrow)$ is assigned to each label using the first entry, b_1, of the seventeen; the remaining bits set the edge label $(b_2...b_{17})_2 \bmod \eta_{nt} \in \Sigma$. To each nonterminal we assign a production of the form

$$Y \rightarrow Z_1...Z_{m_2}$$

where $Y \in \Sigma_m$ is mapped to a sequence of Z_i, each denoted by a bit string $b_1...b_{m_3}$ representing either: a directed non-terminal $X_i \in \Sigma_m$, a terminal $x \in \Sigma$, the empty token λ, or a possible division site $[X_i]$. Observe the homology between biological optimization through cellular division and this parametrization for a truss layout. Organisms begin their development as single cells which develop to some characteristic topology according to biological processes that compile and execute the objectives encoded in DNA. In analogy to this encoding of developmental source over helical structures, the axiom wraps the initial map with directed labels from Σ (acting as the nucleotides) and is matured according to the productions, which are representative of those biological processes actualizing the primordial instructions in DNA; the resulting topology, as opposed to the driving biochemical mechanisms, being of import.

Such are the N_{pop} individuals considered by the $\mathbf{GA}$, which are assigned a fitness value according to

the volume determined from **NP**. In the processing of each fitness evaluation, the axiom is developed to its final state and the initial geometry is supplied. To avoid potential geometric instabilities a constrained Delaunay triangulation is employed to " shore up" the geometry. This operation takes an initial set of points with predefined edges, or regions, and triangulates (produces a grid of triangles) in such a way to maximize the minimal angle of the resulting regions[38]. From an initial, randomly generated, pool of genetic information, the population is subjected to N_{gen} generations of competition according to the selection, crossover, and mutation. Selection is accomplished by the tournament method, which pits m_4 randomly determined individuals against each other until a set percentage of the future generations genetic inheritance is selected; the remaining individuals are chosen from the fittest (elite) of the current generation. A single point crossover, as described in the prequel, is used for mutation. After each crossover step a bit flip operator is applied to each daughter individual. As the name suggests, this operator produces a mutant by assigning to each bit in its binary representation a chance μ that it flips - that is, $0 \rightarrow 1$ or $1 \rightarrow 0$, and are applied to non-elite individuals.

CHAPTER 4
TEST CASES

In this section we examine three structural benchmark problems and provide the optimum framework according to **LP**, **NP**, and **EP**. Aside from Allison's results, we compare **EP** against the benchmark values generated by Achtziger [30] with the Sparse Nonlinear OPTimizer (SNOPT), an implementation of the SQP method developed by Gill et al.[39] that approximates the QP subproblem with a reduced-Hessian algorithm. The eigenresults were determined using the SciPy incarnation of Kraft's [40] Sequential Least SQuares Programming (SLSQP) method, an SQP solver that replaces the quadratic subproblem with a linear least squares subproblem. The results from Wendorff et al., [41] who compared the efficacy of several "off the shelf" nonlinear optimizers for aircraft design, suggest that SNOPT is, in general, a more robust solver than SLSQP, having outperformed all solvers tested and converged in all cases. As such, one expects variance from the benchmark values aside what might be expected from different solvers.

(a)

(b)

(c)

(d)
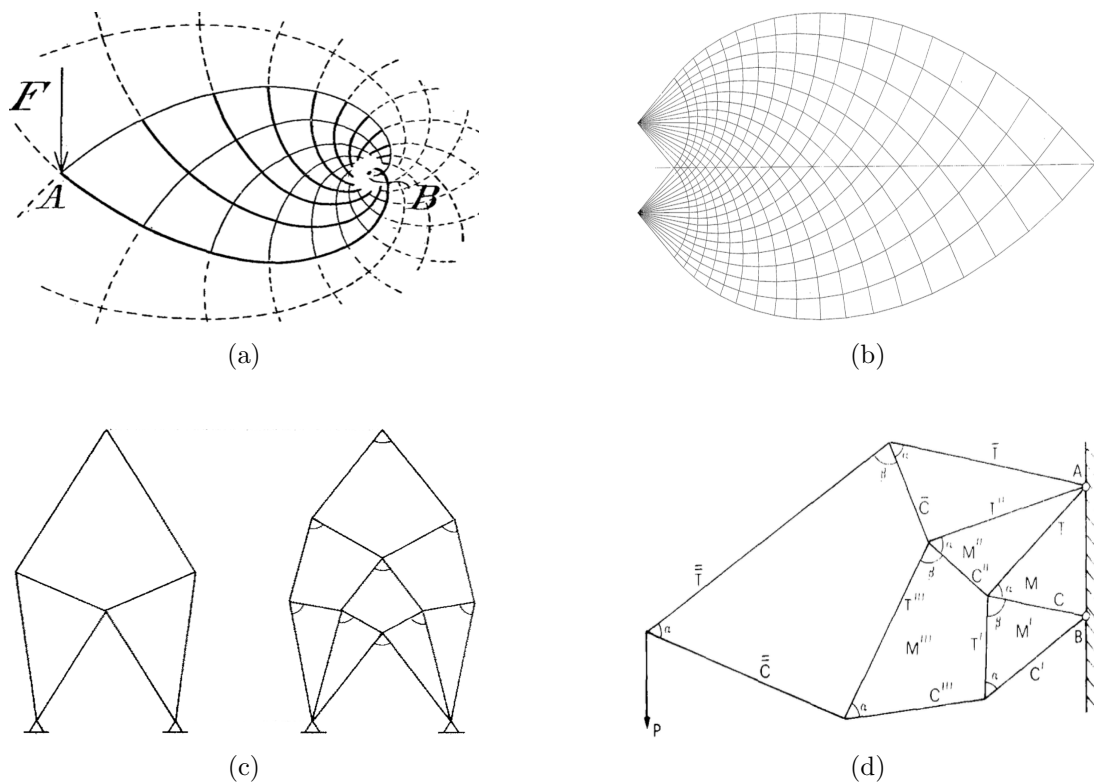
Figure 4.1: Michell optimum cantilevers: (a) the initial case presented by Michell with a single fixed support, (b) the variant solved by Chan with two fixed supports, and Prager cantilevers: (c) $N = 6$ (left) and $N = 11$ (right) node optima for a symmetric cantilever with two pinned supports and a single applied load, (d) optimum non-symmetric cantilever.

The first is a two load cantilever solved by Allison[8] using a method differing from our own in several ways. Because minimum bounds are set on the attainable member areas the basic formulation requires a Sequential Linear Programming (SLP) solution and no global optimum is secured. It ignores direct geometry optimization, or variations of nodal positions, by choosing a parameter $C_{i,j} \in \{0,1\}$ (i and j are two connected vertices) which removes bar $l_{i,j}$ from the system if $C_{i,j} = 0$, completely disregarding a vertex (node) if all members connected to it vanish. This should really be understood in the sense of mobilizing sub-topologies of the initial topology determined from $\omega_{\eta_{dc}}$ - solutions otherwise attained directly by application of **LP**, and thus not necessarily solutions which are optimum with respect to the geometry. To enforce geometric stability the initial map is chosen as a region connecting restrained and loaded joints, as ours, but is pre-divided into triangles. To maintain these triangular regions the allowed production divisions are restricted to compatible sites occurring adjacent to different vertices. A peculiarity in their formulation

$$\min_{\boldsymbol{A},\boldsymbol{C}} \quad \sum \rho C_{i,j} A_{i,j} l_{i,j}$$

$$\text{s.t.} \ \ \sigma_{min} \leq \sigma_{i,j} \leq \sigma_{max}$$

where ρ, $A_{i,j}$, and $l_{i,j}$ are the density, area and length of a member connecting nodes i to j, is the seeming lack of consideration for Newtons equilibrium criteria. It is indicated however, that (allowable) stresses are determined from member areas using the force method solved by SLP iteration.

The second is a finite variant of the optimum cantilever investigated by Michell in which a vertical load applied at a point A is ultimately supported by a force and couple acting on point B a horizontal distance AB from A. The resulting analytical, or Michell optimum, solution is given in Fig 4.1a. Chan[11] concentrated this problem to truss like boundary conditions, considering a similar scenario: two pinned support aligned vertically to accommodate the lack of a flexural capacity in rods (Fig 4.1b), albeit for limited aspect ratios. Observe that no moment is required, and that equilibrium is satisfied by a pair of equivalent forces, either acting on one or the other support. Lewinski et al. extended these solutions to provide optima for all aspect ratios and load directions[42][43]. Pager explored the finite limits of such frameworks using a circle of relative displacement , first for symmetric cantilevers [44], and later extending to the general finite cantilever with a single load and two vertically aligned supports[45][46]. Of particular note is his recognition that Michell optima are arrived at by the limiting case of ideal (weightless) nodes, and that practical optima are determined respective to the node count of the finite structure.

The third is a five load bridge whose exact solution was provided only recently by Lewinski[12] in chapter 7. This result extends Michell's solution for a single load situated between two supports to
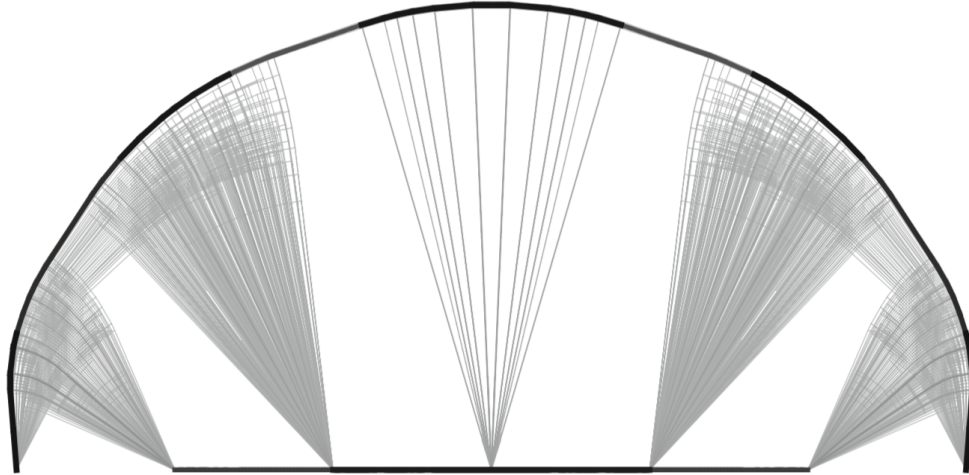
Figure 4.2: Optimum Michell framework for a span of five symmetric loads between two supports.

an arbitrary number of evenly spaced loads. In total, these developments provide minimum bounds for the volumes of the examined frameworks, and suggest the topologies solutions might hope to attain.

Henceforth, all values are normalized and, as such, given without units to simplify the numerical treatment. Each force (member or applied) is taken proportional to a typical applied force F. The member stresses are taken against the stress bound σ, which is equivalent to setting $\sigma = 1$; their areas are non-dimensionalized by the ratio $\frac{F}{\sigma}$; their lengths are scaled by a typical length, l, and is enforced through the ground structure or initial map. and V by the quantity $\frac{Fl}{\sigma}$. A scaled Young's modulus, $E = 1$ is used, and $d = 2$ (as is the case for planar problems) for each.

4.1 The two load cantilever

We consider the scenario described in Fig 4.3a of two vertically applied unit loads, one at coordinate (1,0) and the other at (2,0), and two pinned supports aligned vertically at (0,1) and (0,2). The ground structure consists of a 2×1 grid of $N = 6$ nodes (see Fig 4.3b), each connected to its nearest neighbors for a total $m = 10$ potential members. The initial geometry is collected in the vector $\bar{y} \in \mathbb{R}^{Nd}$, where $Nd = 12$. With two pinned supports there are $n = 2(6 - 2) = 8$ reduced global degrees of freedom, so $f \in \mathbb{R}^8$.

The optimum structure obtained by Allison using the initial map Fig 4.3c is the framework shown in Fig 4.3d, which obtains an actual volume of $V_{SLP} = 15880$ cu-in. Using the stress bound $\sigma = 25$ cu-in, the typical load $P = 100$ kip, and the typical length $L = 360$ in the volume normalized
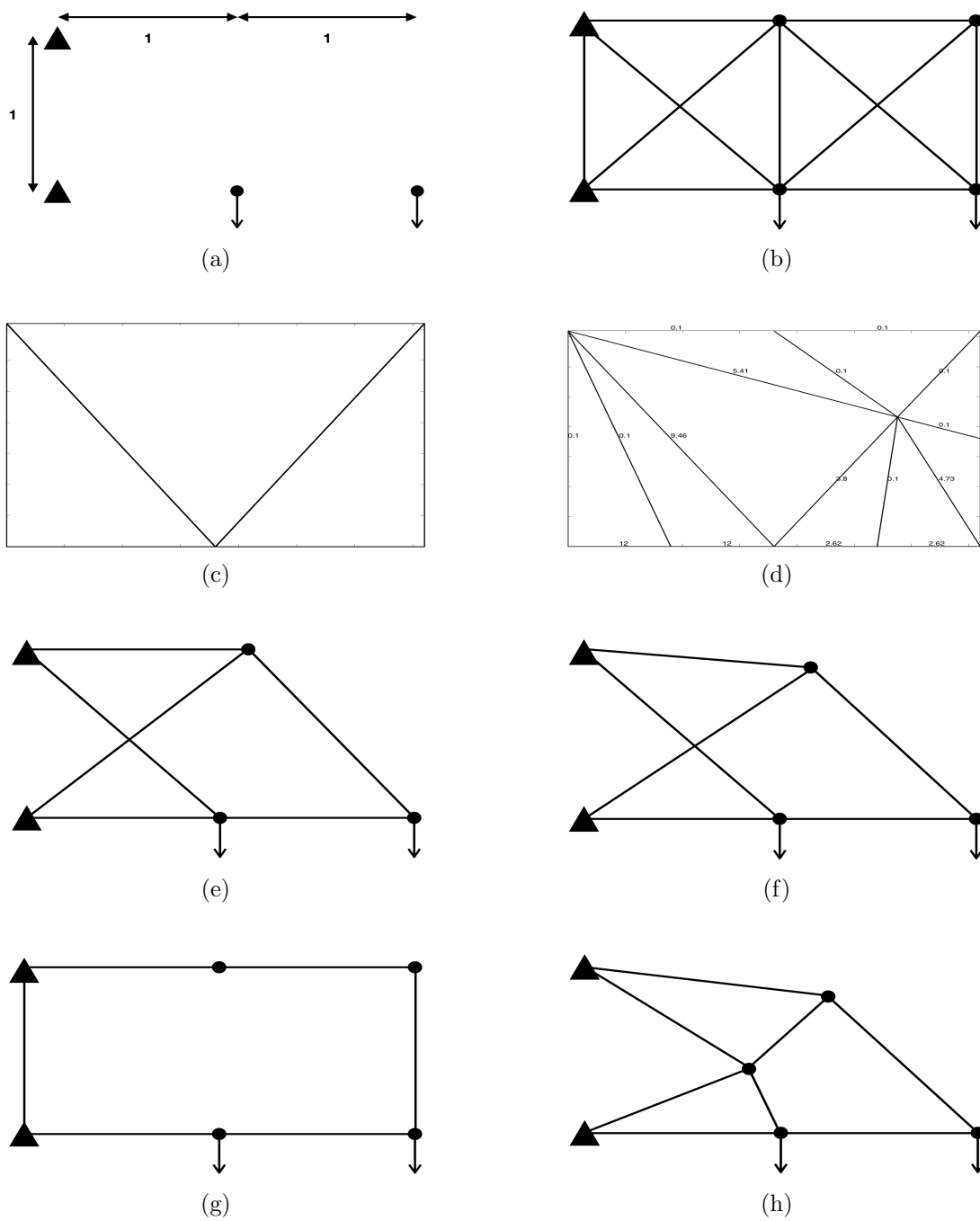
(a)

(b)

(c)

(d)

(e)

(f)

(g)

(h)

Figure 4.3: Two load non-symmetric cantilever: (a) the general structural scenario, (b) the ground structure used for the **LP** and **NP** solutions to the scenario, (c) the axiom used by Allison, (d) the optimum structure generated by Allison, (e) **LP** solution, (f) the **NP** solution, (g) the the initial map applied to conform with the load and restrain sites, (h) the **EP** solution.

25

to $V_{SLP} = 11.03$. By (2.10)-(2.12) the **LP** solution $(\vec{t}', \vec{t}'') \in \mathbb{R}^{10}_+ \times \mathbb{R}^{10}_+$ gives the framework in Fig 4.3e with an optimal, or minimal volume $V = 11.00$. To determine an **NP** solution according (2.22)-(2.25) we stipulate the set of admissible geometries, $Y = \{\boldsymbol{y} \in \mathbb{R}^8 \mid y_p = \bar{y}_p \text{ for } p = n+1, ..., Nd\}$, and commence from the feasible point $(\vec{t}', \vec{t}'', \bar{\boldsymbol{y}})$ towards a KKT point, $(\boldsymbol{t}', \boldsymbol{t}'', \boldsymbol{y}) \in \mathbb{R}^{10}_+ \times \mathbb{R}^{10}_+ \times Y$. According to SLSQP the optimum volume in the nonlinear program is $V_{SLSQP} = 10.7952$. Starting from the initial map Fig 4.3g **EP** determines the minimum structure Fig 4.3h with a a volume $V_{EP} = 10.3741$. This simple solution is 5.95% less than the Allison and **LP** minimums, and 3.90% less than the **NP** solution, which illustrates (in a small way) the gains attainable by **EP**.

4.2   The single load cantilever

We turn to the scenario described in Fig 4.4a of a vertically applied unit load load at coordinate (3,1), and three pinned supports aligned vertically at (0,1), (0,2), and (0,3). The topological domain consists of a 3×2 grid of $N = 12$ nodes (see Fig 4.4b), each connected to its nearest neighbors for a total $m = 27$ potential members. The initial geometry is collected in the vector $\bar{\boldsymbol{y}} \in \mathbb{R}^{Nd}$, where $Nd = 24$. Given three pinned supports there are $n = 2(12 - 3) = 18$ reduced global degrees of freedom, so $f \in \mathbb{R}^{18}$.

The **LP** solution $(\vec{t}', \vec{t}'') \in \mathbb{R}^{27}_+ \times \mathbb{R}^{27}_+$ to this ground structure evidently yields a single framework (reflected in Fig 4.4c&e) with an optimal, or minimal volume $V = 10$. We stipulate the set of admissible geometries, $Y = \{\boldsymbol{y} \in \mathbb{R}^{24} \mid y_p = \bar{y}_p \text{ for } p = n+1, ..., Nd\}$, and start from the linear solution $(\vec{t}', \vec{t}'', \bar{\boldsymbol{y}})$ towards the nonlinear solution $(\boldsymbol{t}', \boldsymbol{t}'', \boldsymbol{y}) \in \mathbb{R}^{27}_+ \times \mathbb{R}^{27}_+ \times Y$. The resulting solutions differ, with that from SNOPT (Fig 4.4d) yielding a smaller optimal volume, $V_{SNOPT} = 9.114$, than that from SLSQP, $V_{SLSQP} = 9.133$, by approximately 0.2%. It is interesting that, where SLSQP converges to and terminates at Prager's symmetric $N = 6$ layout, SNOPT finds the same $N = 6$ solution in one iteration, yet continues to an optimum approaching, but not quite converging to, the symmetric $N = 11$ optimum. Inspecting the whole geometry, so both stressed and zero potential connections, it seems SLSQP only mobilizes nodes 2, 5, and 10; conversely, the sparse method fixes node 8 and varies the remaining free variables. Further numerical investigations reveal this topology is attained by SLSQP only for initial (feasible) geometries in a neighborhood of that optimum. Notice that the SNOPT result is not simple, yet produces a framework of orthogonally intersecting members. It would be interesting to compare those results to SNOPT solution allowing joints at those intersections. The **EP** solution, initial map and structure in Figs 4.4g&h, yields a volume $V_{EP} = 9.120$ - less than SLSQP alone, but not as much as SNOPT.
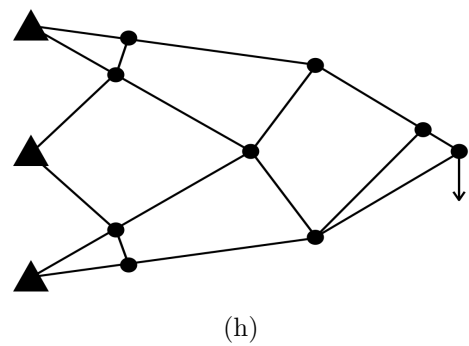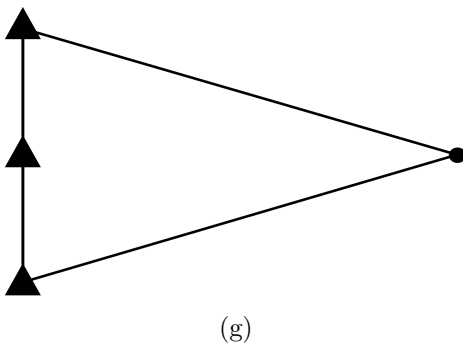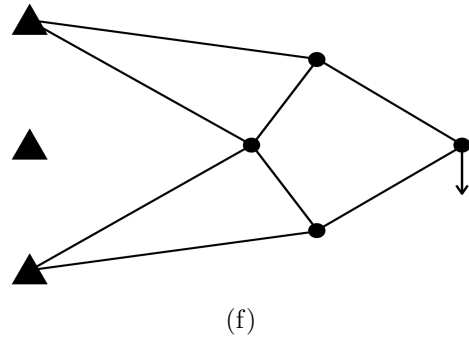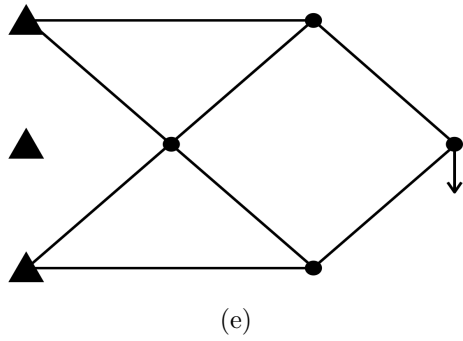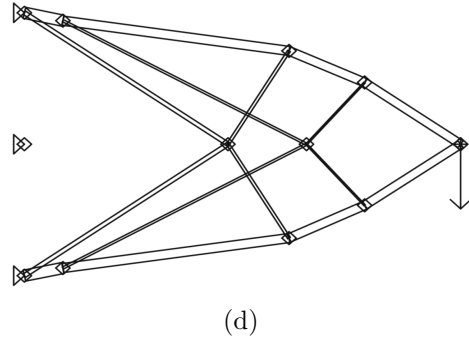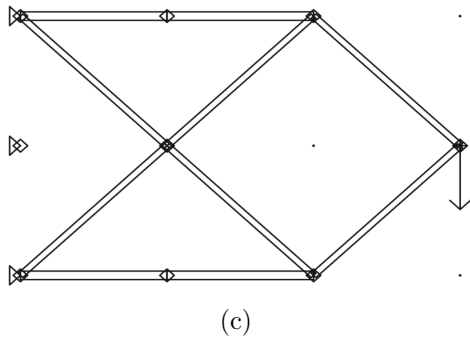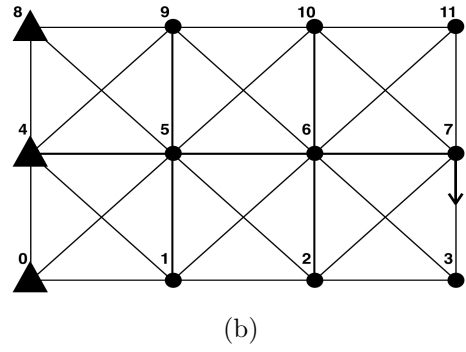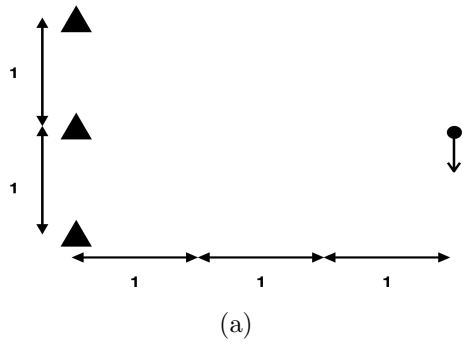
Figure 4.4: Single load symmetric cantilever: (a) the general structural scenario, aspect ratio 1.5, (b) the ground structure used for the **LP** and **NP** solutions to the scenario, (c) **LP** solution using SNOPT, (d) the **NP** solution using SNOPT, (e) the **LP** solution using SLSQP, (f) the **NP** solution using SLSQP, (g) the the initial map applied to conform with the load and restraint sites, (h) the **EP** solution.

27

The volumes obtained by all three methods agree[1] with the lower limit for a symmetric cantilever with 1.5 aspect ratio, $V_{cant,1.5} \approx 9$.

4.3 The five load span

The next scenario (see Fig 4.5a) entails a span of five unit loads evenly spaced on a unit interval between a pinned support (0,0), and a roller (6,0). The domain is set by $N = 12$ nodes arranged in a 6×1 grid (see Fig 4.5b), each connected to its nearest neighbors for a total $m = 33$ potential members. The initial geometry is again collected in a vector $\bar{\boldsymbol{y}} \in \mathbb{R}^{24}$. For a single pinned support and roller there are $n = 2(12 - 1) - 1 = 21$ reduced global degrees of freedom.

LP sizing provides a multitude of solutions $(\vec{\boldsymbol{t}}', \vec{\boldsymbol{t}}'') \in \mathbb{R}^{33} \times \mathbb{R}^{33}$ (two cases are shown in Fig 4.5c&e), each with the same minimal volume, $V = 56$. For simultaneous sizing and geometry optimization we again stipulate the set of admissible geometries, $Y = \{\boldsymbol{y} \in \mathbb{R}^{24} \mid y_p = \bar{y}_p \text{ for } p = 22, ..., 24\}$, and embark from the linear solution. In contrast to the prior scenario, SLSQP yields a solution, $V_{SLSQP} = 34.9881$, which is marginally smaller than the SNOPT value, $V_{SNOPT} = 34.9924$. SLSQP generates a symmetric structure that seems a reasonable extension of the SNOPT estimate. The base geometry suggests this layout is arrived at by sliding node 9 away from 10, towards 8, which disengages member l_{39} and and activates l_{29}, forming the second triangle. Observe that the ground structure disallows topologies with five support triangles, and that both reproduce the vanishing bars l_{01} and l_{56}. The optimum solution generated by **EP**, the initial map and structure given in Figs 4.5g&h, avoids these topological shortcomings, generating a symmetric framework in accords with Fig 4.2 and a superior volume $V_{EP} = 34.6056$, about 1% lighter than either **NP** solution.

The volumes obtained by all three methods agree with the lower limit for a five load span with total length $L_{span} = 6$, that is $V_{span,5} = 34.2284$. So much for spans.

---

[1]For a given aspect ratio the optimum, non-dimensionalized volume is developed by an iterative scheme and plotted in [34]. Due to the quality of our copy, reading for 1.5 gives a volume between 8.8 and 9.0.
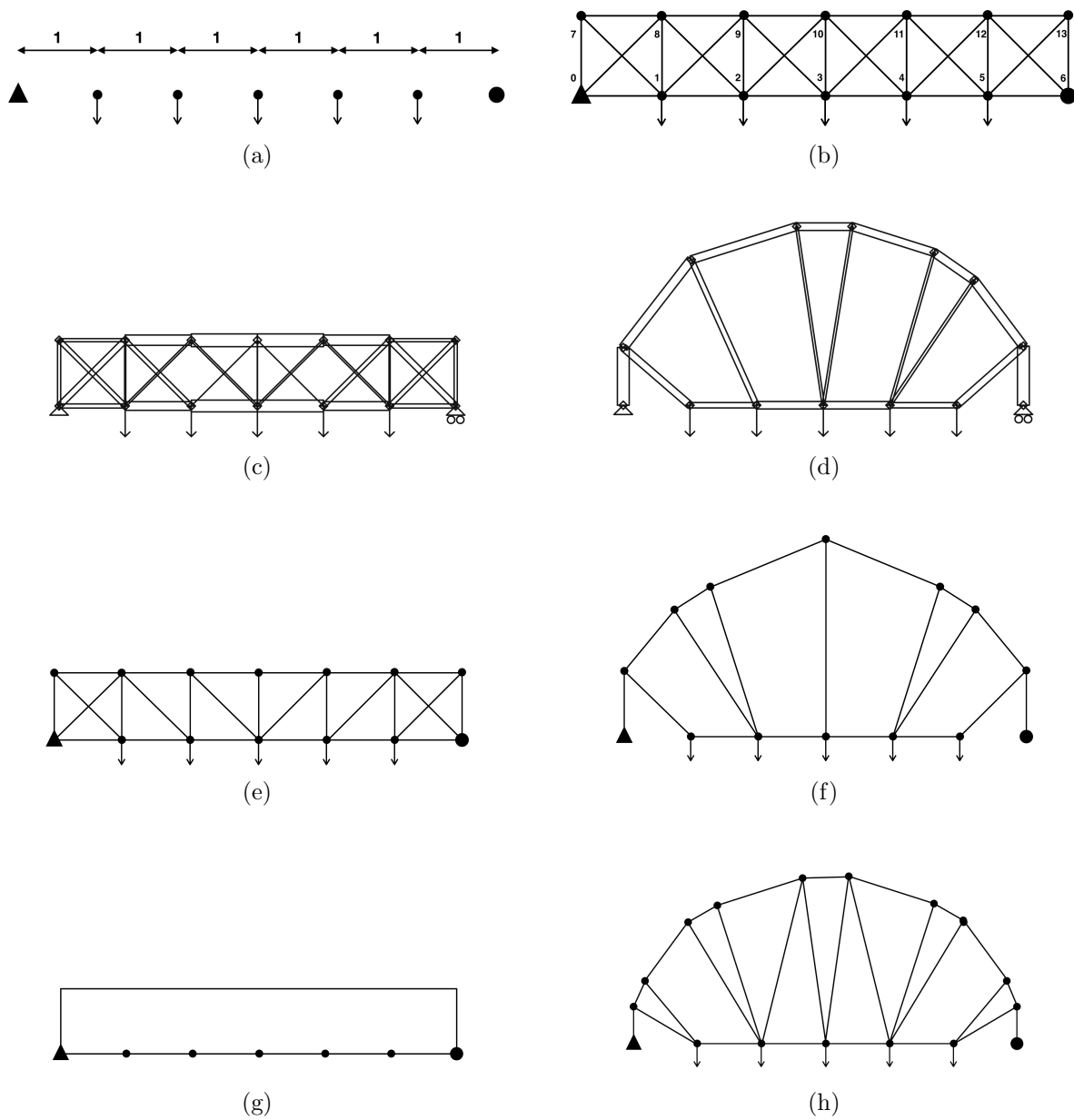
Figure 4.5: The five load span: (a) the general structural scenario, aspect ratio, (b) the ground structure used for the **LP** and **NP** solutions, (c) **LP** solution using SNOPT, (d) **NP** solution using SNOPT, (e) the **LP** solution using SLSQP, (f) the **NP** solution using SLSQP, (g) the the initial map applied to conform with the load and restrain sites, (h) the **EP** solution.

CHAPTER 5
CONCLUSIONS

In the preceding material we have successfully applied Kobayashi's evolutionary programme using map L-systems to optimum truss layouts - that is, sizing, geometry and topology optimization. This method was shown to perform similar or better to the methods employing sparse ground structures, and significantly better than those of Allison, which does not accomplish shape optimization. In addition to this, there are no stipulations on the form of the initial map or the allowed edge connections. In particular, it was seen that certain initial topologies can resist the appearance of optimum structure, and that one should instead search from a less limited pool. We note that a proper testing of this method requires a more complex application than any demonstrated here.

Further work should consider the dynamics of map divisions and the benefits from exploiting symmetries to reduce the required topological search, as well as the inclusion of more realistic constraints for seismic loadings, buckling, and fault tolerance.

BIBLIOGRAPHY

[1] Tero, A., Takagi, S., Saigusa, T., Ito, K., Bebber, D. P., Fricker, M. D., ... & Nakagaki, T. (2010). Rules for biologically inspired adaptive network design. *Science*, 327(5964), 439-442.

[2] Salcedo, M. K., Hoffmann, J., Donoughe, S., & Mahadevan, L. (2018). Size, shape and structure of insect wings. *bioRxiv*, 478768.

[3] Roth-Nebelsick, A., Uhl, D., Mosbrugger, V., & Kerp, H. (2001). Evolution and function of leaf venation architecture: a review. *Annals of Botany*, 87(5), 553-566.

[4] Kobayashi, M. H. (2010). On a biologically inspired topology optimization method. *Communications in Nonlinear Science and Numerical Simulation*, 15(3), 787-802.

[5] Kobayashi, M. H., Pedro, H., & Hude, C. (2009). Topology Optimization Using Map L-Systems. *47th AIAA Aerospace Sciences Meeting including The New Horizons Forum and Aerospace Exposition* (p. 1357).

[6] Pedro, H. T. C., & Kobayashi, M. H. (2011). On a cellular division method for topology optimization. *International Journal for Numerical Methods in Engineering*, 88(11), 1175-1197.

[7] Kolonay, R. M., & Kobayashi, M. H. (2015). Optimization of aircraft lifting surfaces using a cellular division method. *Journal of Aircraft*, 52(6), 2051-2063.

[8] Allison, J. T., Khetan, A., & Lohan, D. J. (2013, May). Managing variable-dimension structural optimization problems using generative algorithms. *The Proceedings of the 10th World Congress on Structural and Multidisciplinary Optimization (WCSMO)*, Orlando, FL.

[9] Maxwell, J. C. (1870). I. On reciprocal figures, frames, and diagrams of forces. *Earth and Environmental Science Transactions of the Royal Society of Edinburgh*, 26(1), 1-40.

[10] Michell, A. G. M. (1904). LVIII. The limits of economy of material in frame-structures. *The London, Edinburgh, and Dublin Philosophical Magazine and Journal of Science*, 8(47), 589-597.

[11] Chan, A. S. L. (1960). *The design of Michell optimum structures*. College of Aeronautics Cranfield.

[12] Lewiński, T. (2018). *Michell Structures*. Springer.

[13] Hemp, W. S. (1973). *Optimum structures*. Clarendon Press.

[14] Christensen, P. W., & Klarbring, A. (2008). *An introduction to structural optimization* (Vol. 153). Springer Science & Business Media.

[15] Martin P.. Bendsøe, & Sigmund, O. (2004). *Topology optimization: theory, methods, and applications.* Springer.

[16] Rozvany, G. I. (Ed.). (2014). *Shape and layout optimization of structural systems and optimality criteria methods* (Vol. 325). Springer.

[17] Rozvany, G. I. N., & Bendsøe, M. P. (1995). Layout optimization of structures. *Applied Mechanics Reviews*, 48(2), 41-119.

[18] Deaton, J. D., & Grandhi, R. V. (2014). A survey of structural and multidisciplinary continuum topology optimization: post 2000. *Structural and Multidisciplinary Optimization*, 49(1), 1-38.

[19] van Dijk, N. P., Maute, K., Langelaar, M., & Van Keulen, F. (2013). Level-set methods for structural topology optimization: a review. *Structural and Multidisciplinary Optimization*, 48(3), 437-472.

[20] Stolpe, M. (2016). Truss optimization with discrete design variables: a critical review. *Structural and Multidisciplinary Optimization*, 53(2), 349-374.

[21] Robinson, R. C. (2013). Introduction to Mathematical Optimization. *Department of Mathematics, Northwestern University*, Illinois US.

[22] Goldberg, D. E. (2006). *Genetic algorithms.* Pearson Education India.

[23] Mitchell, M. (1998). *An introduction to genetic algorithms.* MIT press.

[24] Rajan, S. D. (1995). Sizing, shape, and topology design optimization of trusses using genetic algorithm. *Journal of Structural Engineering*, 121(10), 1480-1487.

[25] Prusinkiewicz, P., & Lindenmayer, A. (2012). *The algorithmic beauty of plants.* Springer Science & Business Media.

[26] Rozenberg, G., & Salomaa, A. (1980). *The mathematical theory of L systems* (Vol. 90). Academic press.

[27] Chomsky, N. (1956). Three models for the description of language. *IRE Transactions on information theory*, 2(3), 113-124.

[28] Chomsky, N., & Miller, G. A. (1958). Finite state languages. *Information and control*, 1(2), 91-112.

[29] Rozenberg, G., & Salomaa, A. (Eds.). (1997). *Handbook of Formal Languages: Volume 1 Word, Language and Grammar.* Springer Science & Business Media.

[30] Hartl, D. J., Reich, G. W., & Beran, P. S. (2016). Additive topological optimization of muscular-skeletal structures via genetic L-system programming. In *24th AIAA/AHS Adaptive Structures Conference* (p. 1569).

[31] Hartl, D. J., Bielefeldt, B., Reich, G. W., & Beran, P. S. (2017). Multi-fidelity analysis and experimental characterization of muscular-skeletal structures optimized via genetic programming. In *25th AIAA/AHS Adaptive Structures Conference* (p. 1442).

[32] Terraz, O., Guimberteau, G., Mrillou, S., Plemenos, D., & Ghazanfarpour, D. (2009). 3Gmap L-systems: an application to the modelling of wood. *The Visual Computer*, 25(2), 165-180.

[33] Bohl, E., Terraz, O., & Ghazanfarpour, D. (2015). Modeling fruits and their internal structure using parametric 3Gmap L-systems. *The Visual Computer*, 31(6-8), 819-829.

[34] Alber, R., & Rudolph, S. (2004). On a grammar-based design language that supports automated design generation and creativity. *Knowledge Intensive Design Technology* (pp. 19-35). Springer, Boston, MA.

[35] Achtziger, W., Bendsøe, M., Ben-Tal, A., & Zowe, J. (1992). Equivalent displacement based formulations for maximum strength truss topology design. *IMPACT of Computing in Science and Engineering*, 4(4), 315-345.

[36] Achtziger, W. (2007). On simultaneous optimization of truss geometry and topology. *Structural and Multidisciplinary Optimization*, 33(4-5), 285-304.

[37] Lindenmyer, A. (1968). Mathematical models for cellular interaction in development, i. filaments with one-sidedinputs, ii. simple and branching filaments with two-sided inputs. *Journal of Theoretical Biology*, 18, 280-315.

[38] The CGAL Project. CGAL. User and Reference Manual, *CGAL Editorial Board*, 4.13 edition

[39] Gill, P. E., Murray, W., & Saunders, M. A. (2005). SNOPT: An SQP algorithm for large-scale constrained optimization. *SIAM review*, 47(1), 99-131.

[40] Kraft, D. (1994). Algorithm 733: TOMP-Fortran modules for optimal control calculations. *ACM Transactions on Mathematical Software* (TOMS), 20(3), 262-281.

[41] Wendorff, A., Botero, E., & Alonso, J. J. (2016). Comparing Different Off-the-Shelf Optimizers' Performance in Conceptual Aircraft Design. In *17th AIAA/ISSMO Multidisciplinary Analysis and Optimization Conference* (p. 3362).

[42] Lewiński, T., Zhou, M., & Rozvany, G. I. N. (1994). Extended exact solutions for least-weight truss layouts, part I: cantilever with a horizontal axis of symmetry. *International Journal of Mechanical Sciences*, 36(5), 375-398.

[43] Lewiński, T., Zhou, M., & Rozvany, G. I. N. (1994). Extended exact least-weight truss layouts, part ii: Unsymmetric cantilevers. *International journal of mechanical sciences*, 36(5), 399-419.

[44] Prager, W. (1977). Optimal layout of cantilever trusses. *Journal of Optimization Theory and Applications*, 23(1), 111-117.

[45] Prager, W. (1978). Nearly optimal design of trusses. *Computers & Structures*, 8(3-4), 451-454.

[46] Prager, W. (1978). Optimal layout of trusses with finite numbers of joints. *Journal of the Mechanics and Physics of Solids*, 26(4), 241-250.